Electronic Supplementary Material (ESI) for Nanoscale.
This journal is © The Royal Society of Chemistry 2016

Supporting information

Dispersal of pristine graphene for biological studies

Arun Prakash Aranaga Raju,[a] Shaun. C. Offerman,[b] Patricia Gorgojo,[a] Cristina Vallés,[a] Elena V. Bichenkova,[b] Harmesh S. Aojula,[b] Aravind Vijayraghavan,[a] Robert J. Young,[a,c] Kostya S. Novoselov,[c,d] Ian A. Kinloch,[a,c,*] and David. J. Clarke[a ,*]

[a]School of Materials, University of Manchester, Oxford Road, Manchester, M13 9PL, UK.

[b]Manchester Pharmacy School, University of Manchester, Oxford Road, Manchester, M13 9PL, UK.

[c]National Graphene Institute, University of Manchester, Oxford Road, Manchester, M13 9PL, UK.

[d]School of Physics and Astronomy, University of Manchester, Oxford Road, Manchester, M13 9PL, UK.

*Corresponding Authors:

ian.kinloch@manchester.ac.uk; david.clarke@manchester.ac.uk

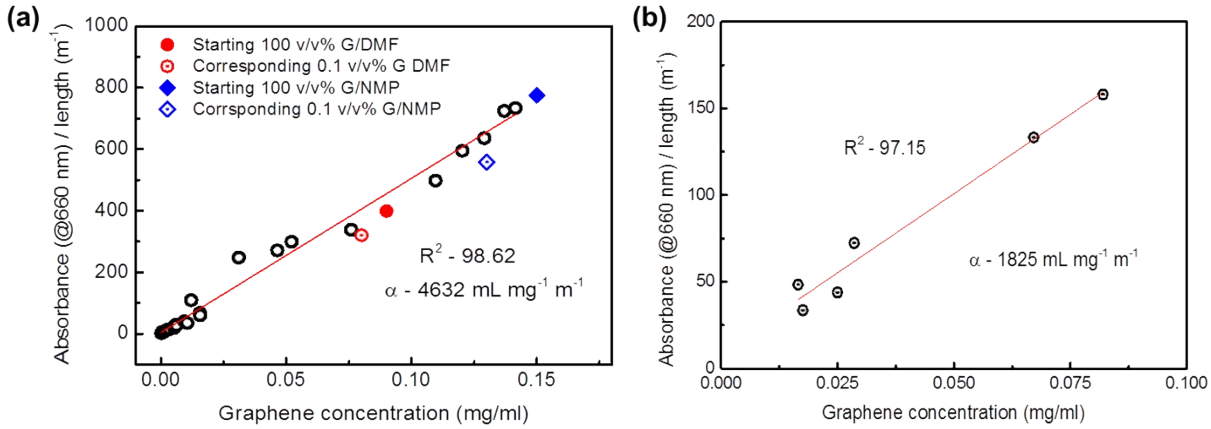

Figure S1: Estimation of absorption coefficients of graphene preparations. The absorption coefficient of graphene is shown to relate to different surface and layer properties of the material. A study conducted by Su *et al.*[S1] on rGO with varying lateral dimensions, mean number of flakes and functional groups, revealed dispersions with smaller flakes (lateral dimension) and fewer layers per flake had lower absorption coefficients, attributed to shrinkage of the π-conjugated systems. They also reported increase in the absorption coefficient with increase in the number of functional groups on the flake due to auxochromic effects.[S1] Given possible variations, concentrations of graphene in the organic solvent **(a)** and aqueous TDOC preparations **(b)** were estimated by gravimetric analysis, which were then used to estimate absorption coefficients, using Lambert-Beer law. Note, each data point is a separate preparation of graphene. Data from example dispersions before and after dialysis (1000 ×) were also added. The slight change in the absorbance value before and after dialysis may be due to a low level of aggregation, but largely represents dilution of graphene during dialysis. The experimentally obtained value of 4632 mL mg^{-1} m^{-1} is very close to the recent theoretically predicted value (4237 mL mg^{-1} m^{-1}) of absorption coefficient of graphene in the visible range,[S2] and was used to calculate the concentration of graphene in dialyzed G/NMP and G/DMF, G/EggPC and G/HSA dispersions.

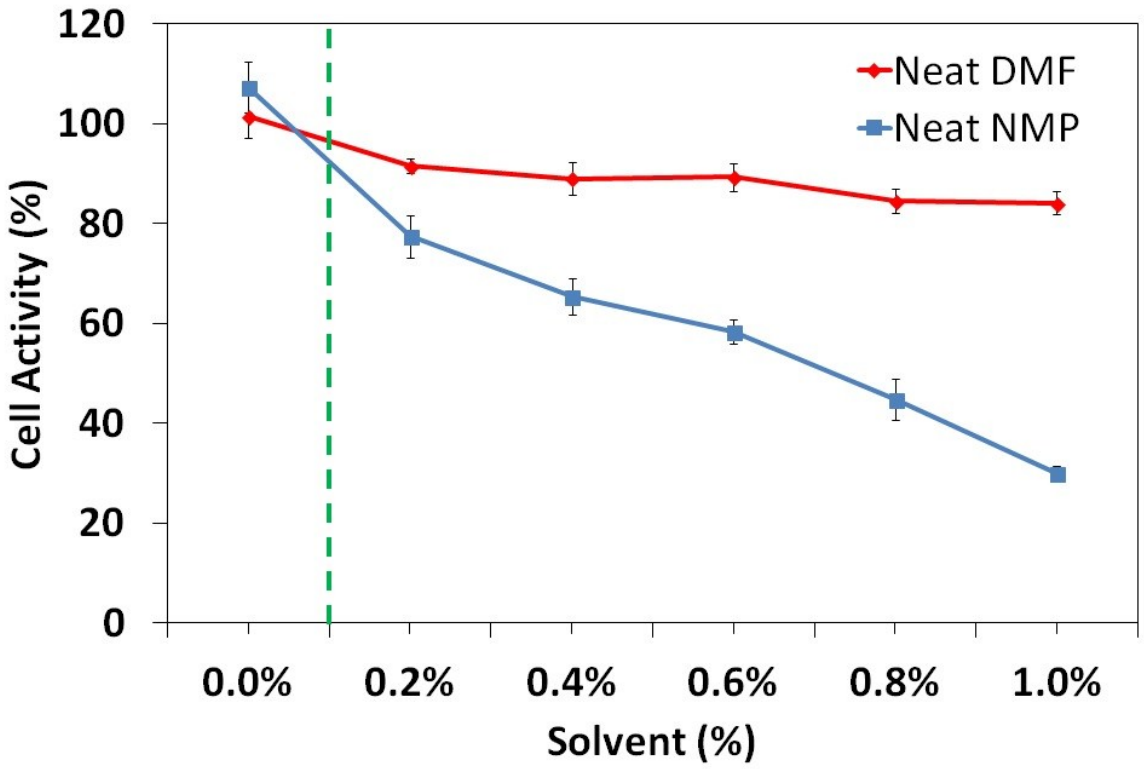

Figure S2: Effect of NMP and DMF solvents on cell metabolic activity

Breast cancer (MCF-7) cells were allowed to adhere overnight to the surface of micro-well plates (Costar 96 well Cell Culture Cluster, Cat No. 3596) at a density of approximately 5000 cells per well, with replicates (n=6), before treatment with graphene preparations diluted into growth medium. Double strength growth medium was prepared from solid medium (Sigma Aldrich, UK. RPMI-R6504. DMEM-D7777) in FCS (100ml) and 1% w/v penicillin/streptomycin (10ml) with sodium bicarbonate (2 g; Sigma Aldrich, UK. S5761) and adjusted to 500 ml with sterile deionized water. Sterile solvent was adjusted to double the concentrations tested with deionized water and mixed with an equal volume of the double strength medium, when 200 µl was added to the adhered cells in each well. After incubation for 24 h at 37 oC under 5% CO2, Resazurin (Sigma Aldrich, UK. 199303) was added (10 µl of 0.1 mg/ml) to each well and the plates further incubated for 6 h, when their fluorescence was read (Ex 570 nm, Em 590 nm, Tecan Safire plate reader). Controls of media only and cells with media were taken as zero and 100% respectively.

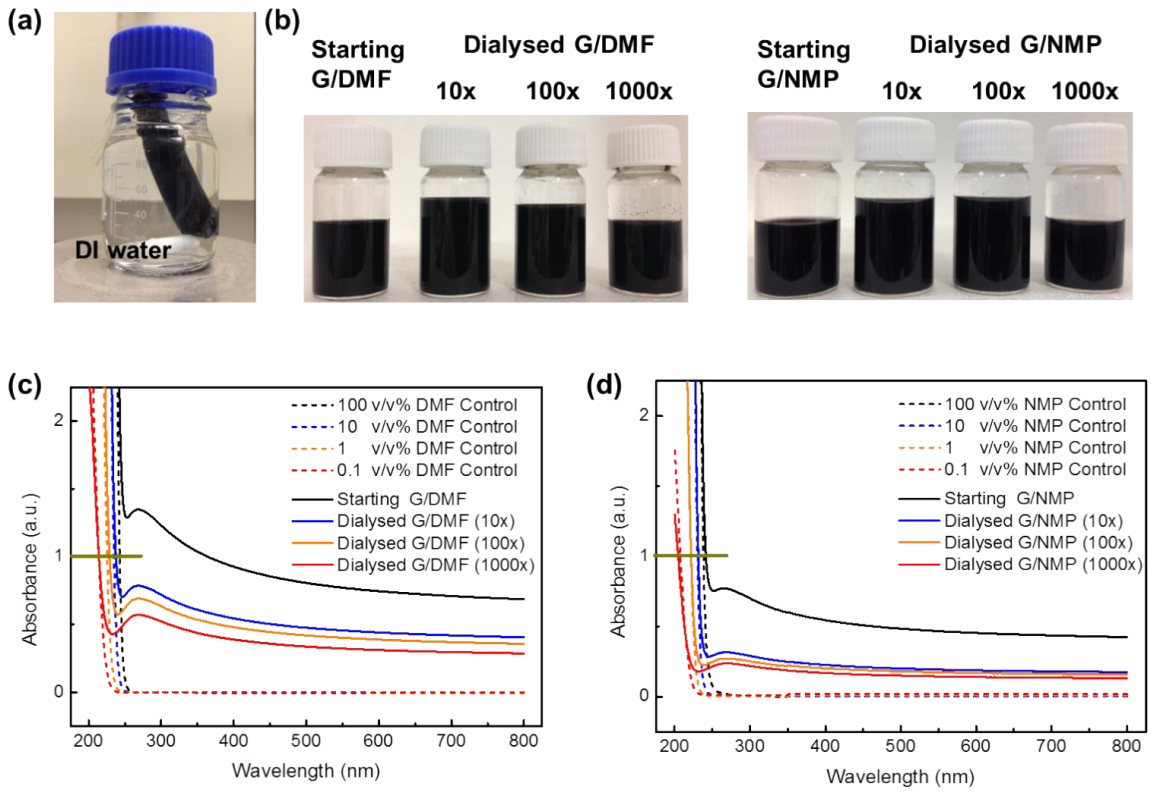

Figure S3: Stable aqueous graphene dispersions by dialysis of graphene produced in organic solvents against deionized (DI) water. Graphene dispersions were produced by bath sonication (Elmasonic P, 32W, 37 kHz, 30% power) of natural graphite (5 mg/ml, grade 2369, Branwell Graphite Ltd. UK) for 60 h in NMP and DMF. Unexfoliated graphite was removed by centrifuging at 4025 ×g for 20 min. The supernatant was further centrifuged at 11180 ×g for 20 min at room temperature, and the pellets were resuspended in 10-15 ml of fresh solvent. Solvent dispersions were introduced into dialysis bags (a) and dialyzed against 3 successive 10 fold volumes of DI water (b), each for 12 h at room temperature, assisted by gentle magnetic stirring. UV-Vis absorbance spectra of diluted (10 fold) dialyzed graphene dispersions (c, d) had similar solvent cut-off wavelengths (solvent absorbance at A=1 compared to control samples of neat solvents in DI water at respective concentrations), suggesting successful dilution of solvents. The absorption at ~269 nm can be attributed to $\pi \rightarrow \pi^*$ transition of the aromatic $C-C$ bonds, indicating that the electronic conjugation within graphene was retained after the dialysis procedure.

Table S1: UV cut-off wavelength of control (DMF and NMP) and dialyzed G/DMF and G/NMP dispersions

Sample (Solvent v/v%)	**UV cut-off wavelength at A=1 a.u. (nm)**			
	DMF Control	**G/DMF (dialyzed)**	**NMP Control**	**G/NMP (dialyzed)**
100 %	242 ± 3	-	238 ± 3	241 ± 3
10 %	234 ± 2	237 ± 2	230 ± 3	231 ± 3
1 %	225 ± 3	228 ± 3	221 ± 2	221 ± 3
0.1 %	213 ± 3	214 ± 3	207 ± 3	204 ± 3

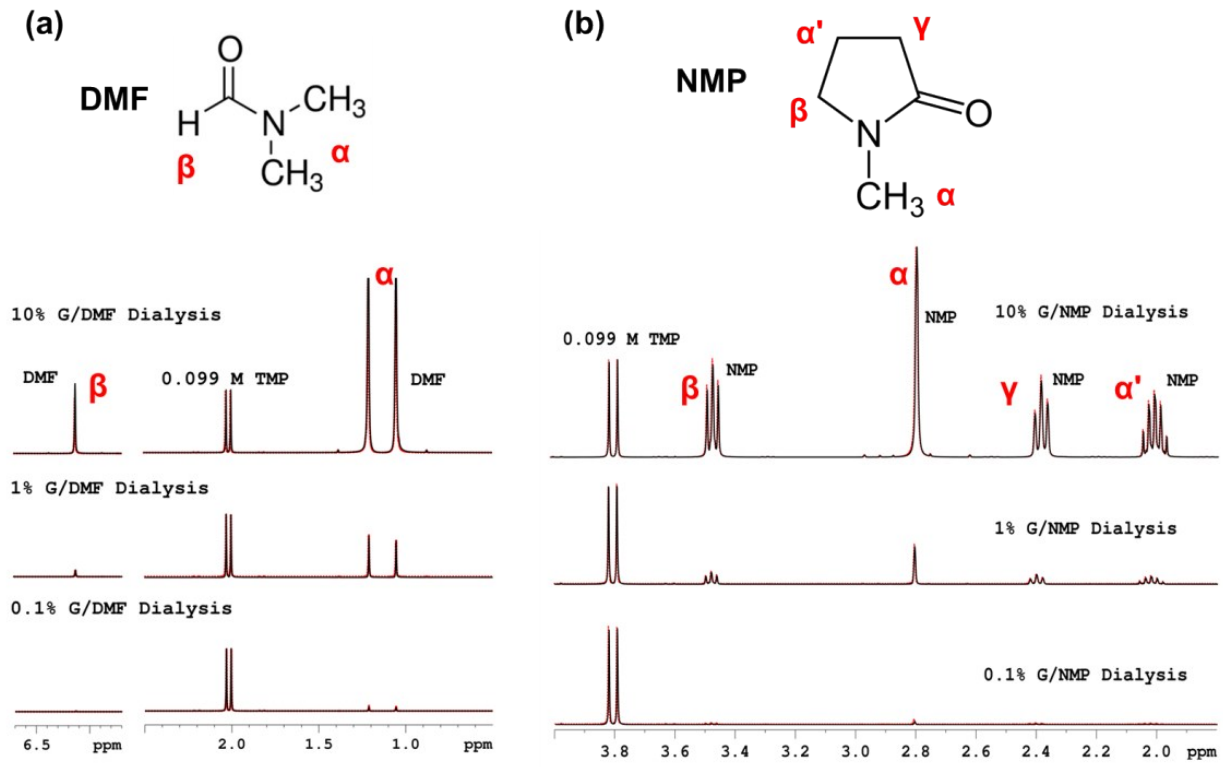

Figure S4: NMR estimation of residual solvents in the dialyzed graphene preparations (400 MHz; Bruker Avance II+). Graphene dispersions were produced by bath sonication (Elmasonic P, 32W, 37 kHz, 30% power) of natural graphite (5 mg/ml, natural graphite, grade 2369, Branwell Graphite Ltd, UK) for 60 h with cooling (temperature held between 22-26 ^{o}C) in NMP and in DMF organic solvents, when both were centrifuged at 4025 × g for 20 min to remove unexfoliated graphite. The supernatants were further centrifuged at 11180 × g for 20 min at room temperature, when the pellets were resuspended in 10-15 ml of fresh solvent. The graphene concentrations in the starting dispersions (G/DMF 0.78 ± 0.02, G/NMP 0.51 ± 0.01) were estimated by absorption at 660nm (4632 mL mg^{-1} m^{-1} absorption coefficient), and each dispersion was dialyzed against heavy water (D_2O) using the same procedure as used for water dialysis. Trimethyl phosphate (TMP, 0.099M) was used as an internal reference in all the dialyzed dispersions. The area under the NMR signals of the chemically-distinct protons of each of the organic solvents was measured by integration

against those generated by –O-$(CH_3)_3$ protons of TMP at known concentrations to estimate the concentrations of organic solvents present in the dispersions. Below are the estimated solvent levels following a typical sequential dialysis of solvent-exfoliated graphene preparations to reduce the solvent level by 10 fold at each dialysis step, and by 1000 fold after 3 dialysis steps against deionized water. Graphene concentrations were also estimated by absorption at 660 nm after each dialysis step.

Table S2: Estimated residual organic solvent levels and graphene concentration of dialyzed dispersions

Dilution of solvent by dialysis (v/v%)	**Solvent level estimated by 1H NMR signal integration (v/v%)**		**Graphene concentration estimated by absorption at 660 nm (mg/ml)**	
	G/DMF	**G/NMP**	**G/DMF**	**G/NMP**
10 × (10 %)	9.64 ± 0.43	8.87 ± 0.44	0.46 ± 0.02	0.21 ± 0.02
100 × (1 %)	0.85 ± 0.04	0.77 ± 0.04	0.41 ± 0.02	0.19 ± 0.01
1000 × (0.1 %)	0.07 ± 0.01	0.07 ± 0.01	0.33 ± 0.02	0.16 ± 0.01

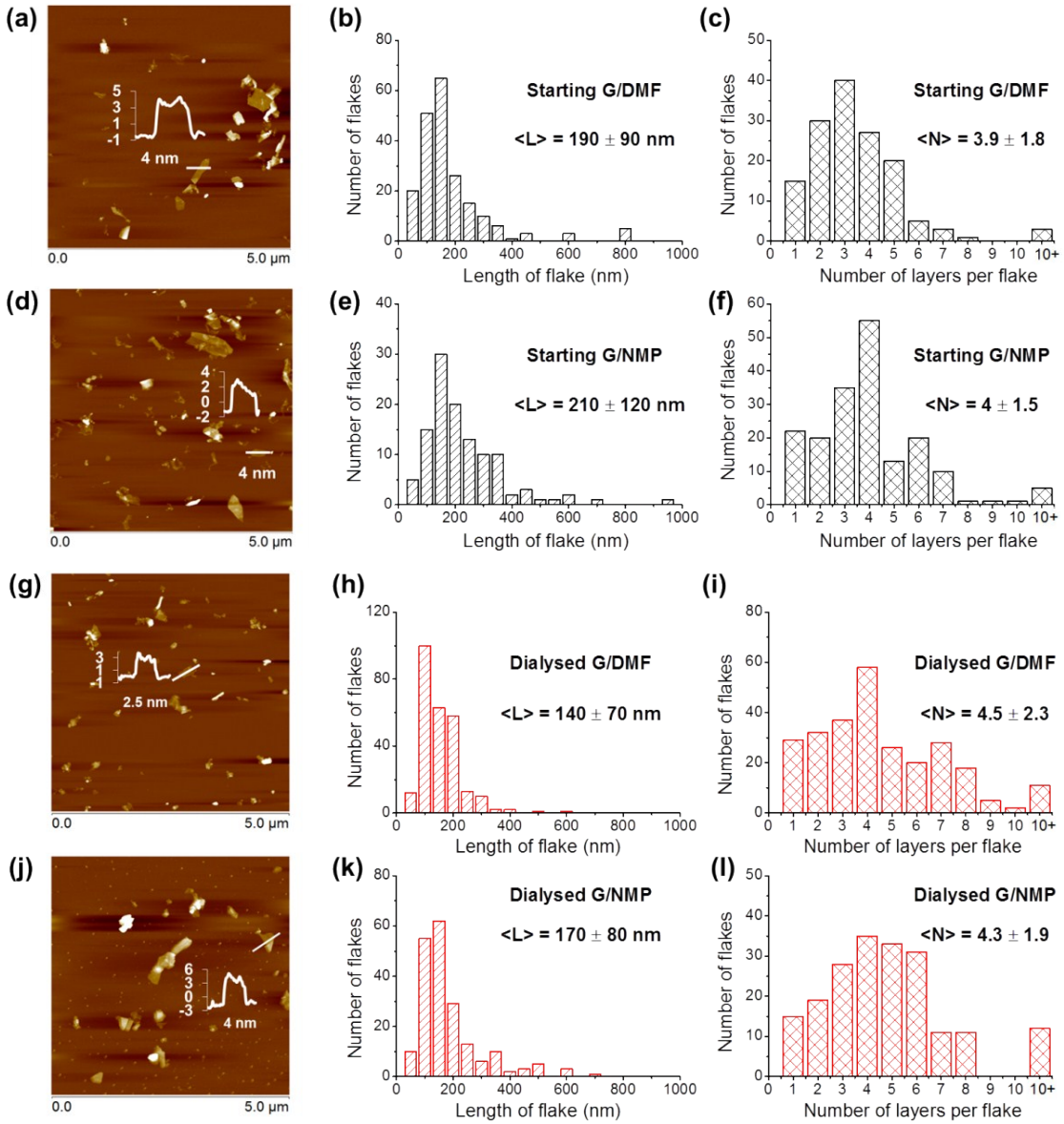

Figure S5: AFM analysis of flake length and thickness of starting and dialyzed (0.1 v/v% solvent) graphene dispersions: representative AFM height scans for (a) starting G/DMF, (d) starting G/NMP, (g) dialyzed G/DMF and (j) dialyzed G/NMP; histograms of the flake length <L> distribution for (b) starting G/DMF, (e) starting G/NMP, (h) dialyzed G/DMF and (k) dialyzed G/NMP; and histograms of the distribution of the number of layers per flake <N> for (c) starting G/DMF, (f) starting G/NMP, (i) dialyzed G/DMF and (l) dialyzed G/NMP.

The mean flake length $\langle L \rangle$ and mean number of layers per flake $\langle N \rangle$ for the dialyzed dispersions were similar to the starting undialyzed dispersions in solvents. Though the mean number of graphene layers per flake was similar (4.5 ± 2.3 for G/DMF and 4.3 ± 1.9 for G/NMP), some shift in the size distribution was apparent indicating slight aggregation. There was a small increase in the number of flakes with more layers (*e.g.,* for $>$ 8 layers, a ~7% increase in $N_{>8}/N_T$, where N_T is the total number of flakes investigated) compared to the starting dispersions. Nevertheless, the proportion of flakes with fewer graphene layers remained similar (*e.g.,* N_1/N_T ~9% and N_{1-5}/N_T ~67%).

Diluted dispersions (~0.5 ml, 10 fold dilution) of starting and dialyzed samples were spray deposited (Evolution Solo Airbrush from Harder & Steenbeck, 1.5 bar Nitrogen gas, 50-100 mm distance, three replicates) on freshly-cleaved mica substrates (pre-heated at 100 ^{o}C). Residual solvents were removed by annealing in a tube furnace under argon atmosphere at 400 ^{o}C for 4 h prior to AFM measurements. Images were recorded in tapping mode using a FastScan-A (Bruker) probe in Bruker Dimension FastScan AFM instrument. All the images were processed in Nanoscope Analysis software.

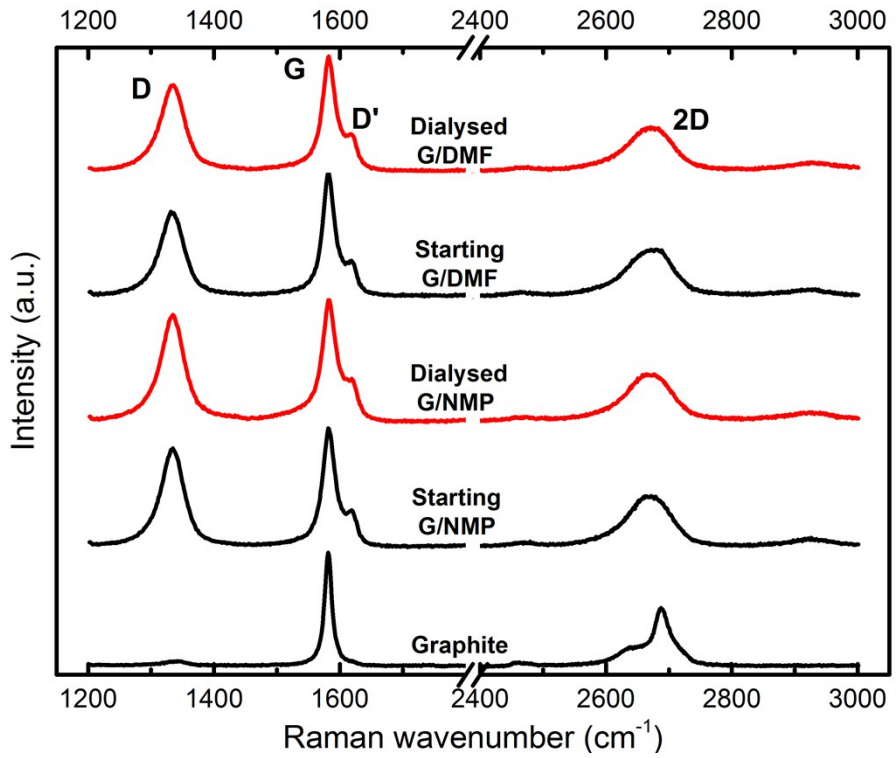

Figure S6: Graphite characteristics and spectral similarity of dialyzed graphene: Raman spectra of dialyzed (red traces) and starting (black traces) graphene exfoliated from graphite (lower trace) in DMF (G/DMF, top two traces) and NMP (middle two traces). The natural graphite powder (Grade 2369 from Branwell Graphite Ltd.) was sieved in 500 mesh to remove any large graphite particles resulting an average lateral dimensions of ~200 µm. The Raman spectra of graphite has single sharp G band at ~ 1580 cm^{-1}, D band at ~1330 cm^{-1} and 2D band at ~2686 cm^{-1} (Two components of 2D band; $2D_1$ ~2636 cm^{-1} and $2D_2$ ~2686 cm^{-1}). The $(I_D/I_G)_{graphite}$ ratio is ~ 0.08 and $\left(I_D/I_{D'}\right)_{graphite}$ ratio is ~ 5. Eckmann *et al.* [S3] studied the nature of defects in graphene by probing the $I_D/I_{D'}$ ratio; ~ 3.5 for boundary type (edge) defects, ~ 7 for vacancy type defects and ~13 for sp^3 type defects. The $\left(I_D/I_{D'}\right)_{graphite}$ ~ 5 for starting graphite suggests presence of some edge or vacancy defects. [S3]

Graphene exfoliated into organic solvents was dialyzed against 1000× volumes of deionized water. Raman spectra were obtained from thin films prepared by vacuum filtering

the dispersions onto aluminium oxide membranes (100 nm pore size, Whatman® anodisc, 100 nm, 47 mm diameter). The dialyzed graphene showed typical Raman bands similar to the starting graphene in solvents: a sharp G band at ~1580 cm^{-1}, a pronounced D band at ~1330 cm^{-1}, a broad and symmetric 2D band at ~2660 cm^{-1}, and shoulder peak, D' band at ~1617 cm^{-1}. The similarity (summarized in the table below) of the position, shape of the 2D band and the peak ratios (*e.g.,* I_{2D}/I_G ~0.5) of the dialyzed dispersions suggest graphene with few layers (< 5) was maintained by dialysis into water. Moreover, the average $I_D/I_{D'}$ ratio of the starting and the dialyzed graphene dispersions are ~ 4 (Table S3), which again confirms the defect type is edge or boundary defects (due to particle size reduction).[S3]

Table S3: Raman spectral characteristics of starting and dialyzed dispersions

Graphene preparation	**Raman 2D position (cm^{-1})**	**FWHM(G) (cm^{-1})**	**FWHM(D) (cm^{-1})**	$\frac{I_{2D}}{I_G}$	$\frac{I_D}{I_G}$	$\frac{I_D}{I_{D'}}$
Starting G/DMF	2669.7 ± 0.6	22.5 ± 0.6	42.1 ± 0.4	0.51 ± 0.02	0.63 ± 0.06	3.92 ± 0.25
Dialyzed G/DMF	2668.5 ± 0.4	23.1 ± 0.5	42.7 ± 0.5	0.45 ± 0.04	0.74 ± 0.02	3.98 ± 0.31
Starting G/NMP	2667.2 ± 0.5	21.5 ± 0.5	43.4 ± 0.3	0.47 ± 0.03	0.81 ± 0.05	4.05 ± 0.17
Dialyzed G/NMP	2667.1 ± 0.6	22.9 ± 0.7	43.3 ± 0.2	0.42 ± 0.06	0.86 ± 0.03	4.24 ± 0.08

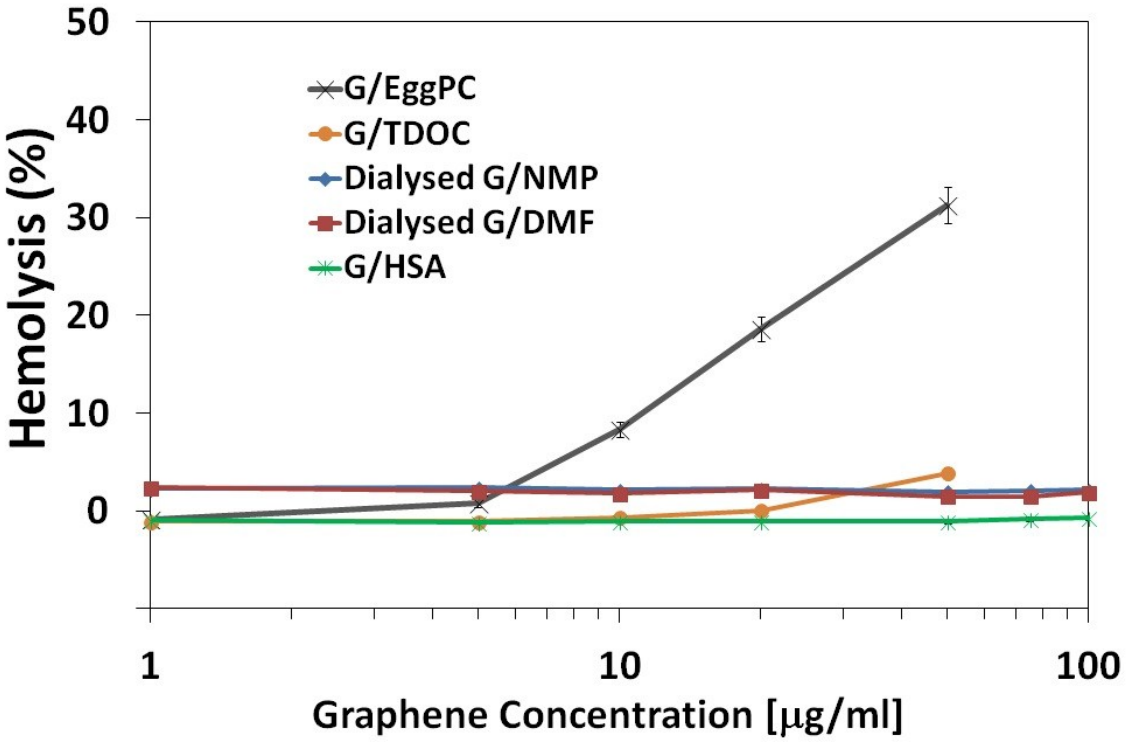

Figure S7: Hemolytic activity of aqueous few layer grapheme preparations.

Defibrinated horse blood (Oxoid Basingstoke UK SR0050C) was centrifuged (100 ×g for 5 min) and the pellet washed in 0.9% w/v NaCl until the supernatant was colorless, when the harvested red blood cells (RBCs) were counted using a hemocytometer and diluted to $5x10^6$ cells/ml. Diluted RBCs (100 µl) were added to replicates (n=4) of each concentration of each graphene preparation (100 µl) and made up to 1 ml with sterile 0.9% w/v NaCl. After incubation at 37 ^oC for 30 min and removal of the RBCs by similar centrifugation, absorbance at 550 nm of aliquots (200 µl) of the supernatants was estimated (Tecan Safire plate reader). Controls of RBCs alone and RBCs treated with surfactant (5% w/v Triton X-100) were taken as 0% and 100% lysis (respectively).

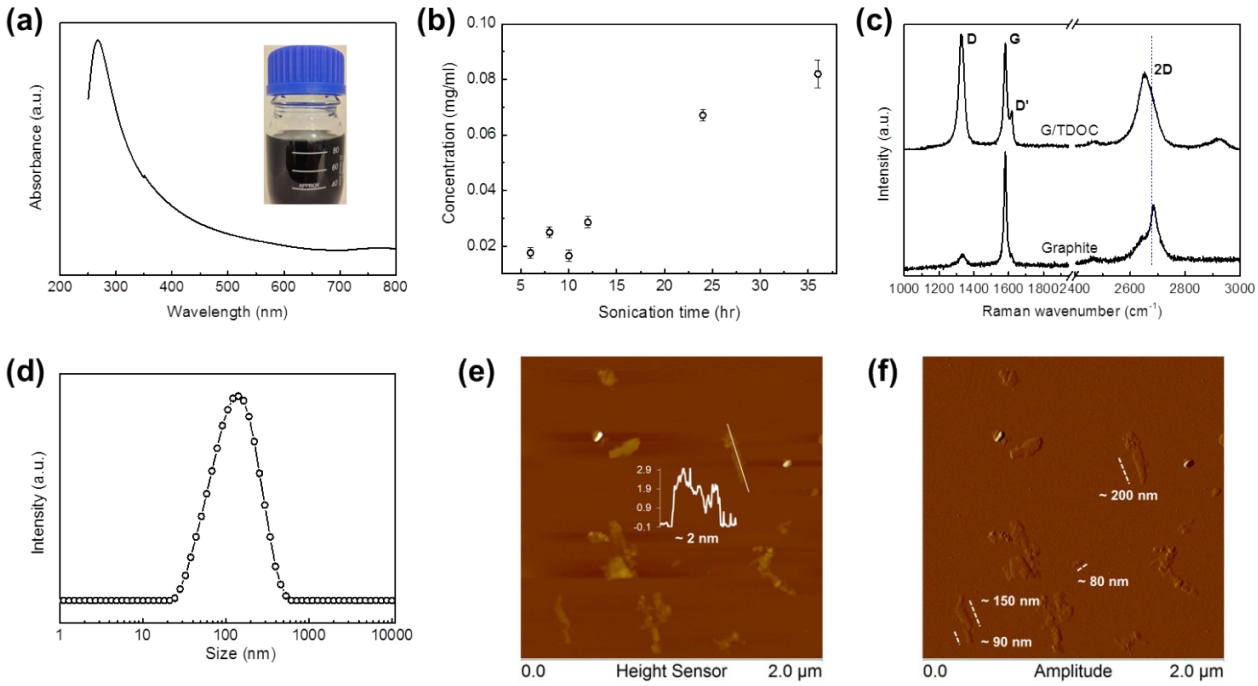

Figure S8: TDOC-exfoliated graphene (G/TDOC) characteristics after 36 h sonication. (a) UV-Vis absorbance spectrum after centrifugation with inset image of the stable dispersion. The strong absorbance at ~269 nm can be attributed to $\pi \rightarrow \pi^*$ transition of the aromatic $C-C$ bonds. (b) Increase in graphene concentration with sonication time (all samples centrifuged at 11180 $\times$g for 20 min). (c) Raman spectra of a thin laminate (by vacuum filtration) of G/TDOC (upper trace) and starting graphite for reference (lower trace). Intensity ratios of the labelled Raman bands were: $I_{2D}/I_G \sim 0.75 \pm 0.06$, $I_D/I_G \sim 1.25 \pm 0.3$ and $I_D/I_{D'} \sim 4.15 \pm 0.3$. (d) Intensity hydrodynamic particle size distribution by DLS, indicating average size ~100 nm. (e) AFM height image with a typical inset height scan used to estimate the average flake length ($\langle L \rangle \sim 90$ nm) and the average number of graphene layers ($\langle N \rangle \sim 3.2$); and (f) corresponding amplitude image, following spray deposition on mica substrates and rinsing with deionized water to remove excess TDOC.

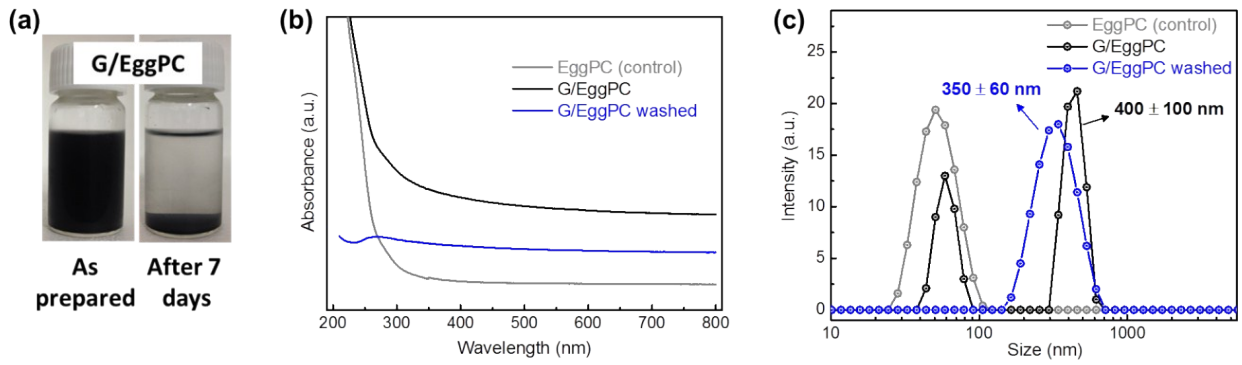

Figure S9: Colloidal stability of lipid-exfoliated graphene. (a) Photographs of stable dispersions (left) and sedimentation observed after 7 days standing at room temperature (right). With shaking and brief (5 min) sonication, the colloidal stability of the dispersion was regained, suggesting weak interactions within the sedimented aggregates. (b) Depletion of lipids from graphene by further washing. The UV-Vis absorption spectrum of lipid-exfoliated graphene (black trace, G/EggPC) showed the UV absorption of the lipids similarly sonicated without graphite (grey trace, EggPC). Upon washing by centrifugation (6708 × g for 10 min), the UV absorption of the lipids was lost, together with about half of the graphene, indicated by the lower graphene absorption in the visible band (blue trace, G/EggPC washed). (c) Size composition of lipid dispersions. Extensively-sonicated lipid films produced small liposomes in the size range 50-100 nm (grey trace, EggPC). Exfoliation of graphene in the presence of sonicated-disrupted liposomes (black trace, G/EggPC) produced a mixed population of small liposomes together with larger 400 nm nanoparticles, presumably lipid associated with graphene. Further washing, removing the small liposomes and lipid visible to UV absorption, showed smaller lipid-depleted graphene of around 350 nm (blue trace G/EggPC washed) indicating weak association between lipid and graphene.

Lipid-exfoliated graphene (G/EggPC) was produced by low power sonication (Elmasonic P, 32W, 37 kHz, 30% power) of natural graphite (250 mg) for ~36 h in 50 ml phosphate-buffered saline (140 mM NaCl) forming liposomes from hydrating lipid films, comprised a

2:1 molar ratio of egg phosphatidylcholine (50 mg) and cholesterol (13.8 mg; G/EggPC). Unexfoliated graphite and large multi-lamellar liposomes were removed by centrifugation (268 ×g for 20 min) and produced the mixed population of small liposomes and lipid-associated graphene (G/EggPC, black traces). Graphene concentrations were estimated by optical absorption at 660 nm using 4632 mL mg^{-1} m^{-1} absorption coefficient (G/EggPC ~0.06 mg/ml).

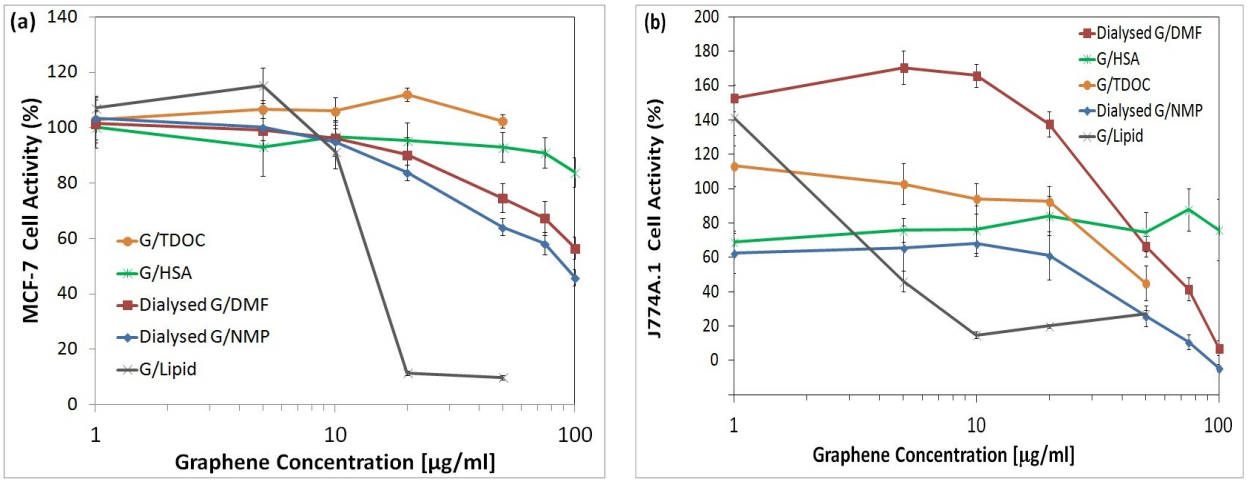

Figure S10: Cell responses to graphene preparations: (a) human breast cancer cells (MCF-7) and (b) mouse macrophages (J774A.1). Cells were incubated with preparations for 24 h at 37 ^{0}C under 5% CO_2, followed by Reazurin for 6 h. Cell activity (%) is scaled against media only (0%) and without graphene (100%). All data is the mean of 4 replicates. Both MCF-7 and J774A.1 cells were allowed to adhere overnight to the surface of micro-well plates (Costar 96 well Cell Culture Cluster, Cat No. 3596) at a density of approximately 5000 cells per well, with replicates (n=6), before treatment with graphene preparations diluted into growth medium. Double strength growth medium was prepared from solid medium (Sigma Aldrich, UK. RPMI-R6504. DMEM-D7777) in FCS (100ml) and 1% w/v penicillin/streptomycin (10ml) with sodium bicarbonate (2 g; Sigma Aldrich, UK. S5761) and adjusted to 500 ml with sterile deionized water. Sterile graphene preparations were adjusted to double the concentrations tested with deionized water and mixed with an equal volume of the double strength medium, when 200 µl was added to the adhered cells in each well. After incubation for 24 h at 37 ^{o}C under 5% CO_2, Resazurin (Sigma Aldrich, UK. 199303) was added (10 µl of 0.1 mg/ml) to each well and the plates further incubated for 6 h, when their fluorescence was read (Ex 570 nm, Em 590 nm, Tecan Safire plate reader). Controls of media only and cells with media were taken as zero and 100% respectively.

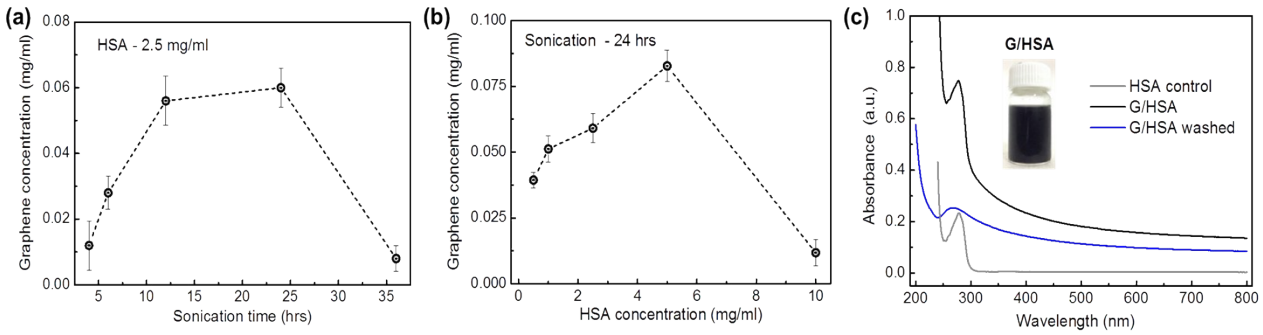

Figure S11: Exfoliation of graphene in albumin. (a) Effect of sonication time on graphene exfoliated in human serum albumin (HSA, 2.5 mg/ml). (b) Effect of HSA concentration on graphene exfoliated for 24 h by bath sonication (Elmasonic P, 32W, 37 kHz, 30% power). Increasing HSA concentration (> 5-10 mg/ml) and sonication time (> 24-36 h) caused albumin aggregation and reduced the graphene concentration, which was estimated by measuring absorbance at 660 nm (α = 4632 mL mg^{-1} m^{-1}). (c) Graphene-adsorbed HSA after washing. Graphene exfoliated in albumin (black trace, G/HSA and inset photograph of the stable dispersion) showed both the typical featureless graphene absorption in the visible band and the UV absorption of amino acids in the HSA (grey trace, HSA control). Washing of the G/HSA by further centrifugation (6708 ×g for 10 min) reduced the UV absorption from HSA, but it was still discernible when the washed pellet was resuspended in the same volume of water (blue trace, G/HSA washed), with some loss of smaller graphene colloid in the supernatant wash.

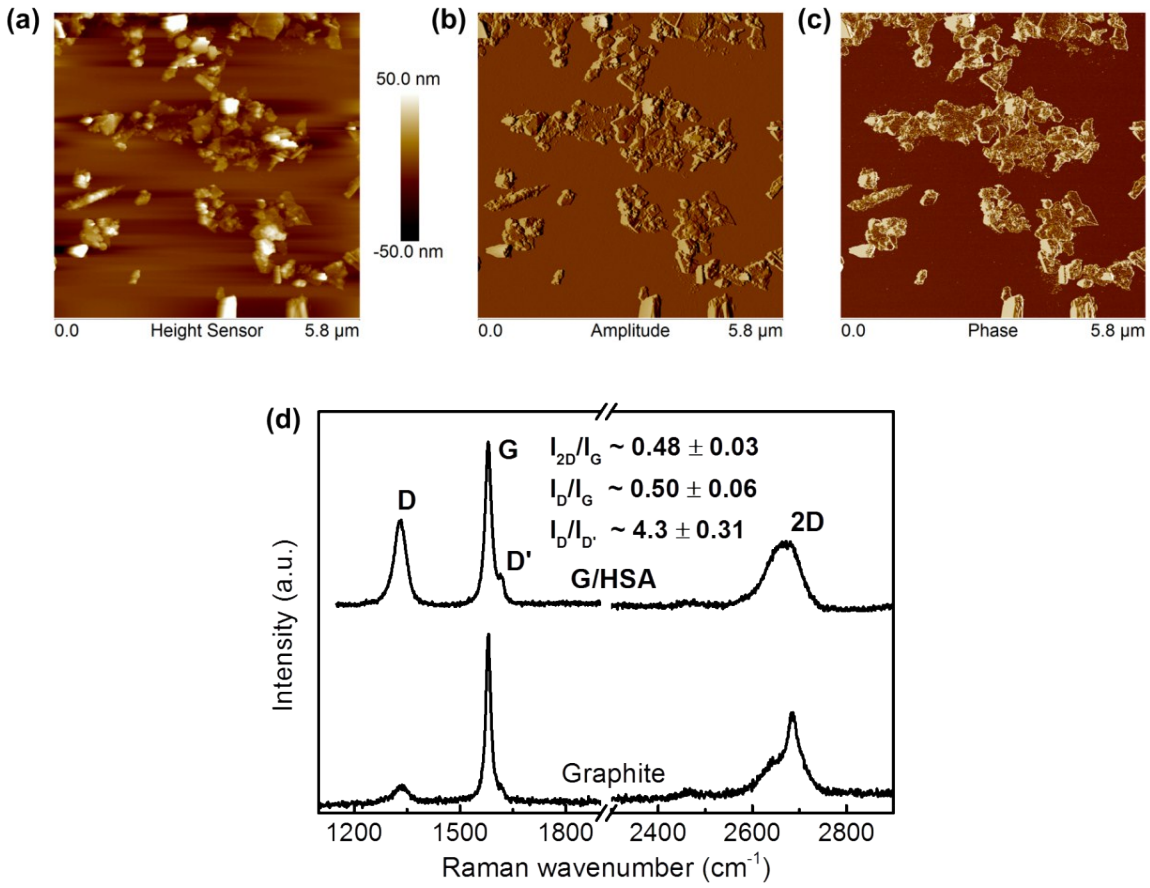

Figure S12: Representative AFM images and Raman spectrum of albumin-exfoliated graphene (G/HSA). Top row: (a) Height sensor image showing a range of G/HSA flakes, (b) corresponding amplitude and (c) images of (a) showing the extent of HSA coverage on the graphene surface. Representative Raman spectra (d) (Reinshaw 2000 spectrometer, 633 HeNe, 1.96 eV, < 1 mW)) comparing starting graphite (lower trace) with graphene-exfoliated in albumin (upper trace, 5 mg/ml HSA). Typical Raman bands were apparent: G band, D band and 2D band. The shape of the 2D band and I_{2D}/I_G ~0.48 ± 0.03 indicates few-layer graphene agreeing with AFM analysis. The presence of D' band with $I_D/I_{D'}$ ~4.3 ± 0.31, with no obvious broadening of FWHM(G) ~21.2 ± 0.5 and FWHM(D) ~41.3 ± 2.1 suggests that the basal plane of graphene was relatively defect free, and the D band with I_D/I_G ~0.5 ± 0.06 was mainly due to edge defects. However, the contribution of adsorbed HSA to the D band of graphene cannot be fully neglected.

REFERENCES

S1. Su, R.; Lin, S. F.; Chen, D. Q.; Chen, G. H. Study on the absorption coefficient of reduced graphene oxide dispersion *J. Phys. Chem. C* 2014, *118,* 12520–12525.

S2. Paton, K.R.; Coleman, J.N. Relating the optical absorption coefficient of nanosheet dispersions to the intrinsic monolayer absorption *Carbon* 2016 (doi:10.1016/j.carbon.2016.06.043).

S3. Eckmann, A.; Felten, A.; Mishchenko, A.; Britnell, L.; Krupe, R.; Novoselov, K. S.; Casiraghi. C. Probing the nature of defects in graphene by Raman spectrocopy *Nano Lett.* 2012, 12, 3925-3930.